

If you wish to distribute this article to others, you can order high-quality copies for your colleagues, clients, or customers by [clicking here](#).

Permission to republish or repurpose articles or portions of articles can be obtained by following the guidelines [here](#).

The following resources related to this article are available online at www.sciencemag.org (this information is current as of August 25, 2010):

Updated information and services, including high-resolution figures, can be found in the online version of this article at:

<http://www.sciencemag.org/cgi/content/full/329/5994/964>

Supporting Online Material can be found at:

<http://www.sciencemag.org/cgi/content/full/329/5994/964/DC1>

This article **cites 26 articles**, 4 of which can be accessed for free:

<http://www.sciencemag.org/cgi/content/full/329/5994/964#otherarticles>

This article appears in the following **subject collections**:

Evolution

<http://www.sciencemag.org/cgi/collection/evolution>

B). Induction of Arc was more rapid and transient, whereas PSD95, GluR1, and synapsin I were delayed, similar to the delay observed after ketamine administration. Lastly, Ro 25-6981 administration produced rapid antidepressant effects (24 hours) in the FST and NSFT, which were blocked by preinfusion (ICV) of rapamycin (Fig. 4, C and D).

Fast activation of mTOR signaling resulting in rapid and sustained elevation of synapse-associated proteins and spine number in the PFC represents a mechanism for the rapid antidepressant actions of ketamine. These effects result in elevated 5-HT neurotransmission, a primary target of traditional antidepressants, although the latter can take weeks or months to induce a therapeutic response (2). The mechanisms underlying the induction of mTOR signaling are unclear, but the requirement for glutamate-AMPA receptor activation is consistent with the hypothesis that there is a subset of NMDA receptors, possibly on γ -aminobutyric acid (GABA)-releasing interneurons,

that when antagonized, block GABA release lead to disinhibition of glutamate signaling (15). Further characterization of these actions of NMDA receptor blockade and the signaling pathways that stimulate mTOR signaling and mediate the rapid induction of synapses in the PFC will provide novel therapeutic targets for antidepressant drug development.

References and Notes

1. R. C. Kessler *et al.*, *JAMA* **289**, 3095 (2003).
2. M. H. Trivedi *et al.*, *Am. J. Psychiatry* **163**, 28 (2006).
3. R. M. Berman *et al.*, *Biol. Psychiatry* **47**, 351 (2000).
4. C. A. Zarate Jr. *et al.*, *Arch. Gen. Psychiatry* **63**, 856 (2006).
5. J. H. Krystal, *Swiss Med. Wkly.* **137**, 215 (2007).
6. Materials and methods are available as supporting material on Science Online.
7. S. Maeng *et al.*, *Biol. Psychiatry* **63**, 349 (2008).
8. C. A. Hoeffer, E. Klann, *Trends Neurosci.* **33**, 67 (2010).

9. Y. Yoshihara, M. De Roo, D. Muller, *Curr. Opin. Neurobiol.* **19**, 146 (2009).
10. R. J. Liu, G. K. Aghajanian, *Proc. Natl. Acad. Sci. U.S.A.* **105**, 359 (2008).
11. E. K. Lambe, G. K. Aghajanian, *Neuroscience* **145**, 900 (2007).
12. G. Rajkowska *et al.*, *Biol. Psychiatry* **45**, 1085 (1999).
13. W. C. Drevets, *Annu. Rev. Med.* **49**, 341 (1998).
14. S. H. Preskorn *et al.*, *J. Clin. Psychopharmacol.* **28**, 631 (2008).
15. N. B. Farber, J. W. Newcomer, J. W. Olney, *Prog. Brain Res.* **116**, 421 (1998).
16. This work is supported by U.S. Public Health Service grants MH45481 and 2P01 MH25642 and by the Connecticut Mental Health Center.

Supporting Online Material

www.sciencemag.org/cgi/content/full/329/5994/959/DC1
Materials and Methods
Figs. S1 to S9
References

31 March 2010; accepted 23 June 2010
10.1126/science.1190287

Females Use Multiple Mating and Genetically Loaded Sperm Competition to Target Compatible Genes

Sarah R. Pryke, Lee A. Rollins, Simon C. Griffith*

Individuals in socially monogamous species may participate in copulations outside of the pair bond, resulting in extra-pair offspring. Although males benefit from such extra-pair behavior if they produce more offspring, the adaptive function of infidelity to females remains elusive. Here we show that female participation in extra-pair copulations, combined with a genetically loaded process of sperm competition, enables female finches to target genes that are optimally compatible with their own to ensure fertility and optimize offspring viability. Such female behavior, along with the postcopulatory processes demonstrated here, may provide an adaptive function of female infidelity in socially monogamous animals.

In socially monogamous species, optimal female mate choice is constrained by the number of high-quality or compatible social partners available. Extra-pair sexual relationships provide an opportunity for females to ensure against the fitness costs of genetically incompatible social partnerships and to improve the genetic quality of at least some of their offspring by mating with extra-pair males that are either genetically more compatible or of higher genetic quality than their social partner (1–3). To date, studies investigating the potential additive genetic benefits provided by extra-pair males have generally either failed to

detect effects or have reported only weak or inconsistent results (4–6). However, most studies have inferred female infidelity through the forensic molecular analysis of the outcome of fertilization (i.e., paternity), and with few exceptions (7), have not considered female copulatory behavior, including the number of partners and the distribution of copulations among them. Therefore, it has been difficult to gain insight into the underlying postcopulatory processes, and ultimately, to determine the adaptive function of female polyandry in socially monogamous animals.

In the socially monogamous Gouldian finch (*Erythrura gouldiae*), genetic incompatibility between interbreeding red and black head-color morphs (that is, different genotypes) results in high offspring mortality rates (more than 60% greater mortality from egg to sexual maturity than compatible pairs of the same head color) (8).

Mate compatibility is signaled by head color, which is determined by a Z-linked gene: Females are hemizygous for this gene (Z^r black, Z^R red), whereas male genotypes can be homozygous Z^rZ^r (black), Z^RZ^R (red), or heterozygous Z^RZ^r (red). Individuals demonstrate precopulatory mate preferences for their own morph type; however, perhaps because of constraints on preferred-mate availability, up to 30% of breeding pairs in wild populations are mixed morph (9).

We tested for adaptive female participation in extra-pair copulations by presenting captive female Gouldian finches breeding in genetically compatible (social partner of the same genotype) and incompatible social pairs (social partner of different morph), with an opportunity to seek an extra-pair copulation with either a compatible or incompatible male (10). On the day after the female-initiated egg laying (day 1; day 0 = day the first egg is laid), the birds in the social pair were physically and visually separated by an opaque divider, which split the cage in half, and a virgin male in breeding condition was placed with the female for 60 min. In the context of selection for compatible genes (1), this experimental design provided a predicted adaptive context (incompatible social partner and compatible extra-pair partner), a maladaptive context (compatible social partner and incompatible extra-pair partner), and two selectively neutral situations (both social and extra-pair partners either incompatible or compatible) (Fig. 1).

Despite morph-assortative mate preferences (9) and selection against mixed morph mating (11), surprisingly, females across all experimental contexts were equally likely to engage in extra-pair behavior [$\chi^2 = 0.87$, degrees of freedom (df) = 3, $P = 0.83$]. Overall, 77.5% (31 of 40) of females copulated with the extra-pair male (Fig. 1). All

Department of Biological Sciences, Macquarie University, Sydney, NSW 2109, Australia.

*To whom correspondence should be addressed. E-mail: simon.griffith@mq.edu.au

successful copulations (i.e., cloacal contact) were preceded by active female solicitation (that is, female orientates cloaca toward male and tail quivers). Only two extra-pair males attempted to force copulations in the 40 trials (5%); females successfully resisted both (i.e., no cloacal contact) and never solicited to these sexually aggressive males. Similarly, forced copulation attempts by social mates were rare (0.6%; 9 of 1398 recorded copulations) and also unsuccessful.

Using characteristic courtship displays (9), potential extra-pair males displayed to females in 95% of the trials (38 of 40 trials). Displays were initiated rapidly [1.71 ± 1.76 (SEM) minutes within introduction to the cage], and males did not discriminate between compatible and incompatible females [i.e., no differences in initiation of singing and courtship behaviors; analysis of variance (ANOVA), $F_{1,38} = 0.39$ to 0.76 , $P = 0.37$ to

0.54]. In six trials, females ignored male displays and did not solicit copulations; in one trial a female solicited, but no successful copulation followed. Most females quickly solicited to extra-pair males (5.32 ± 6.18 min from introduction of the male and within 1.48 ± 1.93 minutes from initiation of male courtship display), irrespective of their own head color (ANOVA, $F_{1,32} = 0.15$, $P = 0.67$) or the extra-pair males' compatibility (head color; ANOVA, $F_{1,32} = 1.98$, $P = 0.18$) or display behaviors (ANOVA, $F_{1,32} = 0.08$ to 1.80 , $P = 0.14$ to 0.78). By participating in extra-pair copulations, extra-pair males can increase their reproductive success with limited investment. In contrast, although a female's participation in extra-pair copulations with a compatible extra-pair male increases the number of eggs she produces [generalized linear model (GLM), $\chi^2 = 3.78$, $P = 0.03$], the female bears the cost of this additional investment, which

may also potentially jeopardize the investment provided by her social partner (12–14). Females may solicit extra-pair copulations with incompatible males because they are unable to always accurately assess male compatibility [for example, red females cannot differentiate between phenotypic red males that are homozygous (compatible) or heterozygous (incompatible) (15)].

Because birds can store sperm from different males for an extended time within their reproductive tract (16), we next examined the potential for postcopulatory sexual selection. As predicted for the outcome of sperm competition for compatible genes (1, 17), the 31 successful extra-pair copulations resulted in a disproportionate number of fertilized offspring among broods ($\chi^2 = 10.10$, $df = 3$, $P = 0.02$) (Fig. 1). Furthermore, after controlling for differences in brood size between the multiple-paternity contexts (Fig. 2), more offspring per brood were fathered by the extra-pair male in the adaptive context than in the two neutral contexts (GLM, $\chi^2 = 12.32$, $P < 0.001$).

Due to the timing of his copulation, the extra-pair male was unable to fertilize the first and second egg, which would have already been fertilized by the social mate; thus, sperm competition between the social and extra-pair males was limited to one to seven potentially fertilizable eggs (i.e., the third to ninth eggs). Within the 14 mixed-paternity clutches, the proportion of extra-pair offspring changed with laying order (GLM, $\chi^2 = 21.2$, $P = 0.004$) (Fig. 2). Similar to other avian studies (18, 19), extra-pair males gained disproportionate fertilization success 24 to 48 hours after copulating, despite females copulating just once (1.28 ± 0.61 ; range = one to two copulations) with most extra-pair males (91.2%) and even though females were in continual contact with their social mates and frequently copulated with them (34.67 ± 7.69 from day -5 to 9), both before (16.22 ± 2.27) and after (18.45 ± 5.45) the experimental extra-pair copulation (Fig. 2). Furthermore, after the extra-pair opportunity (that is, when the social pairs were reunited), 39 of the 40 social males copulated with their female at least once within 30 min of being reunited.

Consistent with the lower value placed on reproductive effort when breeding with incompatible social partners (11), females copulated less frequently with incompatible social mates (1.87 ± 0.14) than with compatible partners (2.75 ± 0.91 ; ANOVA, $F_{1,39} = 6.05$, $P = 0.002$). In particular, females in incompatible social pairings copulated less frequently with their social mates after participating in extra-pair copulations with compatible extra-pair males (i.e., adaptive context; $t = 1.92$, $n = 9$, $P = 0.05$). Nevertheless, the reduced number of social copulations does not explain the greater extra-pair fertilization efficacy (during the period of sperm competition; 2 to 9 days) in this context (Fig. 2C). Compared with the neutral contexts, extra-pair copulations resulted in significantly more extra-pair offspring in the adaptive context ($\chi^2 = 48.43$, $P < 0.001$), and significantly fewer in the maladaptive context ($\chi^2 = 43.21$, $P < 0.001$), than expected from

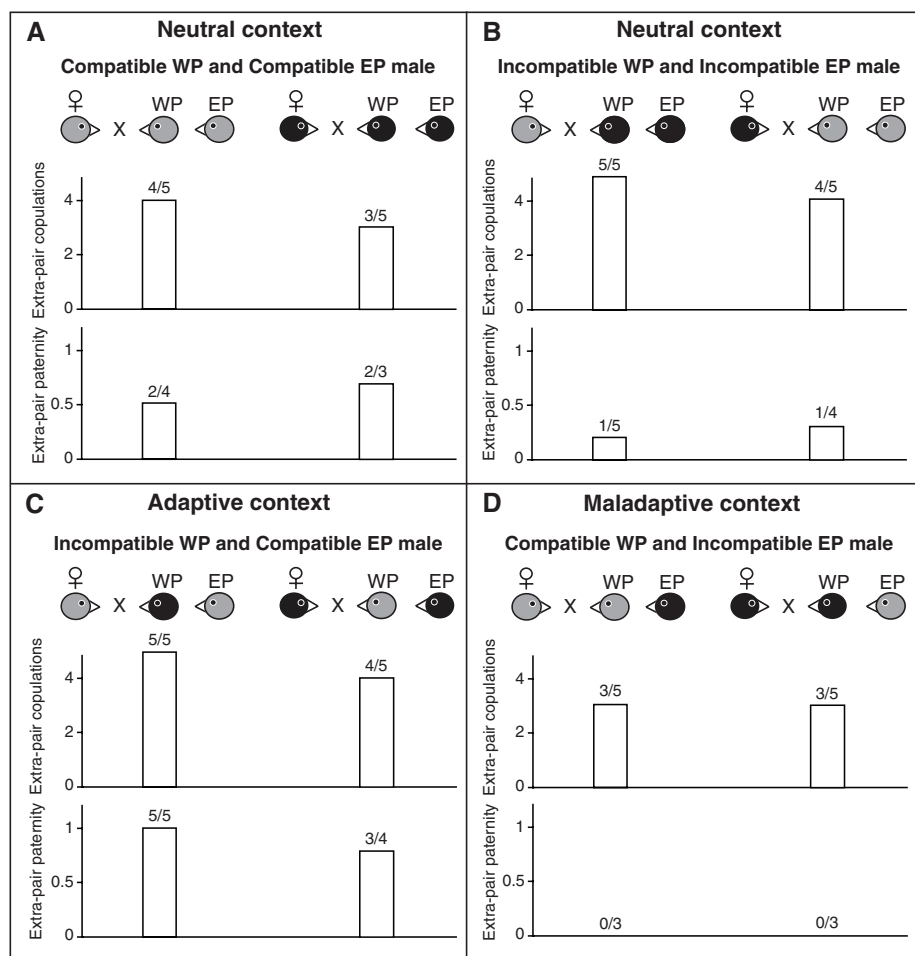


Fig. 1. Across the four experimental contexts, most red (left bars) and black (right bars) females in compatible and incompatible social pairs pursued extra-pair copulations with both compatible and incompatible males. However, resulting fertilization success was highly biased: (A) Four of seven broods and (B) two of nine broods contained extra-pair offspring when both social and extra-pair males were compatible or incompatible; (C) eight of nine broods contained extra-pair offspring when the social male was compatible and extra-pair male was incompatible; and (D) none of the six broods contained extra-pair offspring when the social male was compatible and the extra-pair was male incompatible. WP, within-pair (social) mate; EP, extra-pair mate.

the relative number of extra-pair and social copulations (fig. S1).

We were unable to account for strategic male allocation of insemination size with respect to female quality (19, 20). However, in contrast to previous allocation studies (20), extra-pair males showed equal (and rapid) propensity to mate with both compatible and incompatible females, and virgin extra-pair males (housed in single-sex cages since fledging) were given only this single opportunity to copulate with a female (thus, trade-offs in sperm allocation in lieu of future matings seem unlikely). Although differences in ejaculate size by extra-pair and social males may, in part, explain the disproportional fertilization success of the extra-pair males, the considerable differential

postcopulatory success by extra-pair males across the different contexts demonstrates the extent to which genetic compatibility can bias the outcome of fertilization (Fig. 2).

Although what, and even if, females gain from participating in extra-pair copulations has been debated (4–6), Gouldian finch females seeking extra-pair copulations may ensure fertilization of their eggs by a compatible male and produce more viable offspring. In line with previous results (8), offspring were more likely to survive (from egg to sexual maturity) if their parents were genetically compatible [generalized linear mixed model (GLMM), $\chi^2 = 62.12$, $P < 0.001$], irrespective of whether they were extra-pair or within-pair offspring (GLMM, $\chi^2 = 1.47$, $P = 0.44$). For

females with genetically incompatible social mates, extra-pair copulations with compatible males results in a 38.9% increase in offspring survival, compared to females forced to mate exclusively with their genetically incompatible social mates (8).

Although this system is unusual because of the extent of within-species genetic incompatibility, similar processes may allow females to avoid the negative effects of inbreeding (21–23) and hybridization (24, 25) or to target the positive benefits of heterosis (26). This is likely to be particularly important in systems in which females cannot phenotypically or behaviorally assess compatibility. The cryptic nature of extra-pair copulations (27), as well as the discrepancy between observed extra-pair copulation behavior and the resulting extra-pair paternity, may explain why the adaptive function of female participation in extra-pair copulations has remained elusive (5, 6, 28). The postcopulatory processes demonstrated here may also help to explain previous studies showing variation in intra- and interspecific extra-pair paternity rates (2, 13) and weak or inconsistent differences in quality between extra-pair and within-pair offspring (4, 28). Our findings suggest that, to understand the evolution of female polyandry in socially monogamous animals, we need to account for both pre- and postcopulatory processes. Quantifying all extra-pair copulations and their timing, as well as the strength of selection on genetic compatibility, is challenging. However, our results suggest that neglecting these details may underestimate the extent of behavioral infidelity and the potential adaptive benefits to females.

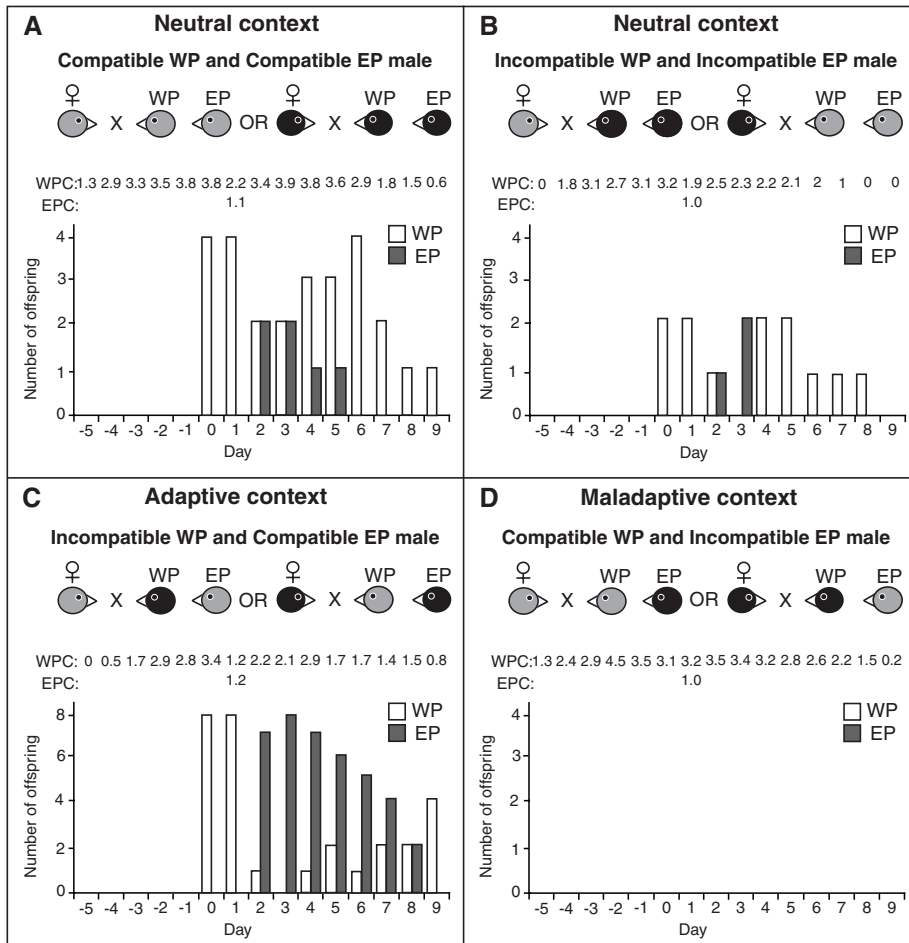


Fig. 2. Extra-pair paternity is determined by the relative genetic compatibility of the WP and EP male with the female. In each predicted context (A to D), the number of eggs fertilized by the social and extra-pair male is shown in laying order, and the average number of copulations each day is provided (above the graph). Conservatively, given that females may store sperm from their social mate (from day -5 to day 1), when both the social and extra-pair males were (A) compatible or (B) incompatible, 4.1 to 5.8% of copulations by the extra-pair male resulted in (A) 28.6% and (B) 27.3% of the offspring produced from the potentially fertilizable eggs (days 2 to 9; extra-pair males were unable to fertilize eggs laid on days 1 and 2). In contrast, (C) 6.1% of copulations by compatible extra-pair males resulted in 76.5% of the offspring produced when the social mate was incompatible, whereas (D) 3.9% of extra-pair copulations by incompatible extra-pair males resulted in no fertilized eggs when the social mate was compatible. WPC, within-pair copulations; EPC, extra-pair copulations.

References and Notes

1. S. C. Griffith, S. Immler, *J. Avian Biol.* **40**, 97 (2009).
2. S. C. Griffith, I. P. F. Owens, K. A. Thuman, *Mol. Ecol.* **11**, 2195 (2002).
3. M. D. Jennions, M. Petrie, *Biol. Rev. Camb. Philos. Soc.* **75**, 21 (2000).
4. E. Açkay, J. Roughgarden, *Evol. Ecol. Res.* **9**, 855 (2007).
5. G. Arnqvist, M. Kirkpatrick, *Am. Nat.* **165** (suppl. 5), S26 (2005).
6. D. F. Westneat, I. R. K. Stewart, *Annu. Rev. Ecol. Syst.* **34**, 365 (2003).
7. A. Cockburn *et al.*, *Behav. Ecol.* **20**, 501 (2009).
8. S. R. Pryke, S. C. Griffith, *Evolution* **63**, 793 (2009).
9. S. R. Pryke, S. C. Griffith, *J. Evol. Biol.* **20**, 1512 (2007).
10. Materials and methods are available as supporting material on Science Online.
11. S. R. Pryke, S. C. Griffith, *Science* **323**, 1605 (2009).
12. T. Albrecht, J. Kreisinger, J. Piálek, *Am. Nat.* **167**, 739 (2006).
13. M. Petrie, B. Kempnaers, *Trends Ecol. Evol.* **13**, 52 (1998).
14. B. C. Sheldon, H. Ellegren, *Proc. Biol. Sci.* **265**, 1737 (1998).
15. S. R. Pryke, *Evolution* **64**, 1301 (2010).
16. T. R. Birkhead, *Adv. Stud. Behav.* **18**, 35 (1988).
17. M. A. Ball, G. A. Parker, *J. Theor. Biol.* **224**, 27 (2003).
18. T. R. Birkhead, J. Pellatt, F. M. Hunter, *Nature* **334**, 60 (1988).
19. N. Colegrave, T. R. Birkhead, C. M. Lessells, *Proc. Biol. Sci.* **259**, 223 (1995).

20. T. Pizzari, C. K. Cornwallis, H. Løvlie, S. Jakobsson, T. R. Birkhead, *Nature* **426**, 70 (2003).
21. M. Olsson, R. Shine, T. Madsen, A. Gullberg, H. Tegelstrom, *Nature* **383**, 585 (1996).
22. A. Pusey, M. Wolf, *Trends Ecol. Evol.* **11**, 201 (1996).
23. T. Tregenza, N. Wedell, *Nature* **415**, 71 (2002).
24. J. Merilä, L. E. B. Kruuk, B. C. Sheldon, *Nature* **412**, 76 (2001).
25. T. Veen *et al.*, *Nature* **411**, 45 (2001).
26. J. Merilä, B. C. Sheldon, S. C. Griffith, *Ann. Zool. Fenn.* **40**, 269 (2003).
27. W. G. Eberhard, *Female Control: Sexual Selection by Cryptic Female Choice* (Princeton Univ. Press, Princeton, NJ, 1996).
28. S. C. Griffith, *Am. Nat.* **169**, 274, discussion 282 (2007).
29. We thank T. Birkhead, R. Brooks, R. Calsbeek, S. Immler, S. Ulfstrand, D. Westneat, and M. Whiting for comments on the manuscript. This work was supported by Discovery Grants DP0770889 (S.R.P.) and DP0881019 (S.C.G.) from the Australian Research Council, a L'Oréal for Women in Science Fellowship (S.R.P.), and the Save the Gouldian

Fund. The Animal Care and Ethics Committee of Macquarie University approved this research.

Supporting Online Material

www.sciencemag.org/cgi/content/full/329/5994/964/DC1

Materials and Methods

Fig. S1

Table S1

References

17 May 2010; accepted 7 July 2010
10.1126/science.1192407

Cell Lineage Reconstruction of Early Zebrafish Embryos Using Label-Free Nonlinear Microscopy

Nicolas Olivier,^{1*} Miguel A. Luengo-Oroz,^{2*} Louise Duloquin,^{3*} Emmanuel Faure,⁴ Thierry Savy,⁴ Israël Veilleux,¹ Xavier Solinas,¹ Delphine Débarre,¹ Paul Bourguine,^{4,5} Andrés Santos,² Nadine Peyriéras,^{3,6†} Emmanuel Beaurepaire^{1†}

Quantifying cell behaviors in animal early embryogenesis remains a challenging issue requiring in toto imaging and automated image analysis. We designed a framework for imaging and reconstructing unstained whole zebrafish embryos for their first 10 cell division cycles and report measurements along the cell lineage with micrometer spatial resolution and minute temporal accuracy. Point-scanning multiphoton excitation optimized to preferentially probe the innermost regions of the embryo provided intrinsic signals highlighting all mitotic spindles and cell boundaries. Automated image analysis revealed the phenomenology of cell proliferation. Blastomeres continuously drift out of synchrony. After the 32-cell stage, the cell cycle lengthens according to cell radial position, leading to apparent division waves. Progressive amplification of this process is the rule, contrasting with classical descriptions of abrupt changes in the system dynamics.

Although classical developmental biology is characterized by qualitative descriptions, recent work underlines the requirements for precise measurements to enable formal reconstruction integrating the genetic, molecular, and cellular levels of organization (1–3). The optimization of microscopy imaging techniques and improved data algorithmic processing are key issues in such reconstructions. Parallelized linear microscopy such as light-sheet fluorescence microscopy provides fast imaging but suffers from loss of information with depth (4). Point-scanning two-photon microscopy provides deeper imaging (5) but exhibits slower frame rate, compromising

automated individual cell tracking in whole organisms (6). Furthermore, the usual implementation of these two paradigms does not allow homogeneous illumination in spherical samples, leading to a difficult tradeoff between the detection of deep structures and illumination-induced perturbation in outer layers. Finally, relying on fluorescent staining of biological structures brings additional artifacts and limitations. Exploiting the intrinsic optical nonlinear properties of the sample is a valuable, although challenging, alternative. Second-harmonic generation (SHG) is obtained from dense noncentrosymmetric structures such as oriented microtubule assemblies (7–9), including mitotic spindles (8, 10). Third-harmonic generation (THG) is obtained from optical heterogeneities (11)—such as the interface between an aqueous medium and a lipidic, mineralized, or absorbing structure (12)—and allows morphological imaging of small organisms (10, 13).

Here, we show that combining SHG and THG imaging of unlabeled embryos with a scanning scheme matching embryo morphology provides adequate three-dimensional (3D) imaging over time for the automated reconstruction of cell behavior during zebrafish embryo cleavage stages (14). Ad hoc image analysis strategies for cell position, division, and shape identification were used to produce a complete and validated lineage

tree for a cohort of six zebrafish embryos until the 1000-cell stage, annotated with minute-level division timing, micrometer-accuracy cell coordinates, and shape characteristics. These data provided a quantitative spatiotemporal description of the wave-like division cycles and allowed the construction of a prototypic digital blastula. The cycle duration of sister cells exhibited variability that did not correlate with cell volume, revealing unexpected cell division asynchrony and asymmetry from the first division cycles and leading to increasing cell heterogeneity by the time of midblastula transition (MBT) (14).

An appropriate image acquisition scheme was devised to provide high-resolution time-lapse imaging of intrinsic SHG and THG signals (Fig. 1 and supporting online material). Excitation in the 1.2- μm range reduced nonlinear endogenous absorption by the sample and allowed simultaneous two-photon-excited fluorescence (2PEF) imaging of red fluorescent proteins (Fig. 1, B and C) for control experiments. When imaging a spherical embryo, scattering and aberrations typically result in reduced signal at the center of each plane (Fig. 1E). We therefore scanned each plane of a half-sphere along a spiral trajectory with variable speed to spend more time imaging the innermost cells (Fig. 1, D to F, and fig. S1). This conformal strategy provided optimal acquisition time and minimal photoperturbation (fig. S2). SHG and THG signals were co-optimized by using rotating linear incident polarization. In addition, because THG contrast from a specific structure depends on its size relative to the focal volume (15), moderate focusing (3.5- μm Z-resolution) was used to highlight cell interface compared with smaller subcellular structures (Fig. 2D).

Combining the conformal scanning scheme described above, sensitive detection, infrared excitation wavelength, and appropriate focusing and polarization conditions allowed homogenous detection of mitotic spindles and cell and tissue phenotypic features in the whole unlabeled zebrafish embryo during cleavage stages. The blastoderm was contained in a half sphere of 440- μm radius imaged with a temporal resolution of 80 s and a volumetric pixel size of 2 by 2 by 4 μm , suitable for further automated reconstruction of the cell lineage tree.

The intrinsic THG signal revealed a number of structures and dynamic processes (Fig. 2, A to J, and movies S1 to S6) and highlighted cell contours even better than membrane staining by

¹Laboratory for Optics and Biosciences, Ecole Polytechnique, CNRS, INSERM, Palaiseau, France. ²Biomedical Image Technologies, Universidad Politécnica de Madrid, and Biomedical Research Center in Bioengineering, Biomaterials, and Nanomedicine (CIBER-BBN), Madrid, Spain. ³Neurobiologie et Développement, Institut de Neurobiologie Alfred Fessard, CNRS, Gif/Yvette, France. ⁴Centre de Recherche en Epistémologie Appliquée, Ecole Polytechnique, CNRS, Paris, France. ⁵Réseau National des Systèmes Complexes, 57-59 rue Lhomond, Paris, France. ⁶Institut des Systèmes Complexes Paris Ile-de-France, 57-59 rue Lhomond, Paris, France.

*These authors contributed equally to this work.

†To whom correspondence should be addressed. E-mail: nadine.peyrieras@inaf.cnrs-gif.fr (N.P.); emmanuel.beaurepaire@polytechnique.edu (E.B.)